JOURNAL OF Materials CHEMISTRY

Crystal structures and molecular mechanics calculation of nonlinear optical compounds: 2-cyclooctylamino-5-nitropyridine (COANP) and 2-adamantylamino-5-nitropyridine (AANP). New polymorphic modification of AANP and electro-optical effects

Mikhail Yu. Antipin,*[a,b] Tatiana V. Timofeeva,[a] Ronald D. Clark,[a] Vladimir N. Nesterov,[a] Fedor M. Dolgushin,[a,b] Javier Wu[c] and Alex Leyderman[c]

[a]*Department of Chemistry, New Mexico Highlands University, Las Vegas, New Mexico, 87701, USA*
[b]*Institute of Organoelement Compounds, Russian Academy of Sciences, 28 Vavilov St., B-334 Moscow, Russia*
[c]*Department of Physics, University of Puerto-Rico at Mayaguez, P.O. Box 9016, Puerto-Rico*

Received 19th July 2000, Accepted 2nd November 2000
First published as an Advance Article on the web 13th December 2000

A new polymorphic modification (space group $Pca2_1$, $Z=4$) obtained by crystallization from acetonitrile solution has been discovered for 2-adamantylamino-5-nitropyridine (AANP), a prospective NLO material. This new phase is isostructural with the known crystal structure of 2-cyclooctylamino-5-nitropyridine (COANP) and is characterized by the optimal molecular orientation for the highest effective NLO responses in the solid state. On the contrary, AANP crystals obtained from the melt or vapor phase belong to another space group $Pna2_1$ ($Z=4$) and have less optimal molecular orientation for NLO responses. New accurate single crystal X-ray diffraction data including low-temperature data were obtained for both compounds (COANP and two phases of AANP). It was found that at room temperature the structure of COANP is characterized by a crystal disorder related to the flexibility of the cyclooctyl ring, but no new crystal phases were found for this compound. For both compounds molecular mechanics calculations of the molecular conformations have been performed, together with calculations of the crystal packing and crystal morphology. Both linear and quadratic electro-optical effects of COANP and AANP crystal films were examined by an ac modulation method using a longitudinal setup, and the electrooptical coefficient r_{51} and figures of merit were estimated and compared.

Introduction

Organic nonlinear optical (NLO) materials have been the subject of very intensive studies in the last few years because of their potential applicability in image processing and optical communications. Owing to the very large molecular optical nonlinearities related to highly delocalized π-electron states in molecules, very fast optical response times and higher optical damage thresholds as compared with the well known inorganic materials, organic compounds offer several application advantages for electronic devices.[1–3] Among the most attractive features of these materials is the possibility of optimizing their optical properties using molecular and crystal engineering methods.[4,5] Crystal acentricity and "optimal" molecular packing of organic chromophores (*i.e.* their dipole moment or charge transfer orientations with respect to the polar crystal axes) are amongst the few necessary requirements in such a design for the manifestation of large NLO responses, in particular for second harmonic generation (SHG) or electro-optical (EO) effects in the solid state.[1–3,6]

The known strategy in molecular and crystal engineering of solid NLO materials is synthesis of organic chromophores with chiral centers. This approach guarantees that crystallization of a pure enantiomer will occur in a non-centrosymmetric space group, although molecular chirality itself is not the only necessary factor providing crystal acentricity. For example, formation of some motifs of the intermolecular hydrogen bonds in crystals between the achiral molecules results in some cases in non-centrosymmetric crystal structures.[7,8] On the other hand, the fact that the molecule of interest is optically pure does not guarantee that the corresponding crystal packing array will be adequate for NLO effects, *i.e.* molecular packing in the crystal may not be "optimal" for manifestation of the highest or desirable NLO responses in the solid state. Therefore some other chemical modifications of organic chromophores are widely used in the synthesis of NLO materials. In particular, the introduction into a molecule of inactive bulky groups is one such method of modification.[6]

It is known that NLO chromophores are very often highly polar in their ground states, therefore it is reasonable to expect that the dipole–dipole interactions between polar molecules would favor antiparallel head-to-tail packing, and hence lower NLO characteristics even in the case of acentric crystals. (We must note however that, though common, this idea is not supported in general by some detailed studies, see for example ref. 9.) In order to reduce the probability of antiparallel (usually centrosymmetric) packing, a number of molecules in which neutral bulky groups alternate with the hyperpolarizable moiety have been prepared.[10–12] Following this idea a large series of 2-amino-5-nitropyridine derivatives with different bulky substituents at the amino-nitrogen atom have been obtained to demonstrate the workability of this approach in NLO crystal engineering.[10–15]

The most thoroughly investigated representative of this series is 2-cyclooctylamino-5-nitropyridine (COANP) which forms non-centrosymmetric orthorhombic crystals (space group $Pca2_1$) and has excellent NLO properties in the solid state.[10*a*,*b*,14] This compound was first described as a new prospective NLO material in 1987 (see ref. 10*a*), and in a number of more recent publications[10*b*,14,16–18] its NLO

DOI: 10.1039/b005822j

characteristics and thermal behavior have been studied in detail. It was found,[16] for example, that COANP exhibits an anomalous solidification upon cooling from the melt which allows for the formation of a poling induced non-centrosymmetric glassy state exhibiting pronounced second harmonic generation and large nonlinear optical susceptibilities.

Apart from the importance in fabrication of optically nonlinear glassy thin films for guided wave optics, COANP is interesting as it allows one to study the freezing transition and the formation of the glassy state at very slow cooling rates below 1 K min^{-1}; in particular, for COANP this state was found to exist for several months.[16] Nevertheless, despite the importance of COANP as an NLO material, its structural studies are rather scarce. Single crystal X-ray diffraction data published in ref. 10*a* were not accurate enough by present-day standards, and contained only minimal crystallographic information without any analysis of the molecular geometry, crystal packing and atomic displacement parameters that might be important for understanding thermal properties of this compound having a flexible cyclooctane fragment in its molecule.

Many other derivatives of 2-amino-5-nitropyridine as well as 2-amino-5-nitropyridinium salts have also been found to possess SHG properties in the solid state, forming "optimal" or close to optimal herringbone motifs in their crystals.[11–15] Therefore, this fragment may be considered as a good "synthon" for NLO crystals engineering. Among these derivatives are (−)-2-(α-methylbenzyl)-5-nitropyridine,[12] numerous salts of the 2-amino-5-nitropyridinium cation with different inorganic anions ($H_2PO_4^-$, $H_2AsO_4^-$, $CHCl_2COO^-$, Cl^-, Br^-, $HO_3PCH_2COO^-$, and some others, see refs. 13–15), and the very close "relative" of COANP, 2-adamantylamino-5-nitropyridine (AANP). The last compound was found to be a very active solid NLO material, its relative SHG intensity is about 300 times of that of urea.[19,20] However, X-ray structural data for AANP (as well as for COANP) contained only minimal information about unit cell parameters, space group ($Pna2_1$), and partial molecular packing.[11] Information about the crystal structure and atomic coordinates of AANP is even absent in the Cambridge Crystallographic Database (Release 2000). The lack of structural data for these important compounds makes difficult a comparative analysis of these structures as well as comparison and optimization of their NLO responses. Therefore a detailed crystallographic analysis of these similar materials would be of special interest for understanding the nature of their NLO properties and their possible optimization and application.

Another important approach in the discovery of new NLO crystals is a systematic search for NLO-active polymorphs using different methods of single crystal growth (crystallization from different solvents and/or under different conditions, from melts, vapor phase, *etc.*). Although polymorphism is sometimes an undesired phenomenon in crystal growth, the existence of polymorphic forms is significant and interesting. It provides an opportunity to obtain new NLO-active forms and also to investigate the molecular-orientation–crystal property relationship, as well as the growth kinetics–thermodynamic relation. In the case of polymorphism, the molecular packings are different, so crystal parameters, for example refractive indexes and tensor components of nonlinear optical coefficients which are very important in the design of NLO materials, are also different. So, there is a possibility that a suitable (and maybe more NLO-active) polymorph may be chosen according to the type of NLO device by changing the crystal growth conditions or methods. We must note, however, that such a polymorph would need to be at least metastable.

There are only a few examples in the literature devoted to a study of new crystal forms of organic NLO compounds or to a selective growth of polymorphs.[21–25] In particular, two NLO-active forms (both having acentric space groups $P2_12_12_1$ and $Pna2_1$) were found for the organic chromophore 8-(4′-acetylphenyl)-1,4-dioxa-8-azaspiro[4.5]decane (APDA) using the melt growth and plate sublimation techniques.[23] In the study of 5-nitrothiophene-2-carbaldehyde 4-methylphenylhydrazone (NTMPH)[24] three polymorphs were found by crystallization in various solvents at different conditions, and one of these phases was found to be acentric (space group $Pna2_1$). Some other examples of polymorphism in NLO materials are presented in Ref. 25*a*,*b*. It seems quite probable that the number of possible polymorphic modifications for a given compound is very often more than one, and the main problem is to find appropriate conditions for crystal growth. An excellent review on polymorphism in organic crystals was published very recently.[25*b*]

In the present paper we report a detailed X-ray diffraction analysis of the molecular and crystal structures and polymorphism of COANP and AANP. We directed our efforts to a search of new possible polymorphic phases of these compounds using different techniques for crystal growth. We expected that polymorphism of COANP might be related to the conformational flexibility of the cyclooctane ring in this molecule that has been demonstrated in our earlier publication.[26] However, no new crystalline phases were found for this compound. The only manifestation of the molecular flexibility for COANP is the probable formation of a glassy state on cooling the melt which results in a crystal structure disorder at room temperature. To reveal the nature of this disorder (static or dynamic) in the present work we collected X-ray diffraction data for COANP at two temperatures, 297 and 167 K, respectively.

On the contrary, for the AANP we found two crystal phases, including one that was previously unknown. It was found that the $Pna2_1$ phase published earlier[11] may be obtained from the melt (see also ref. 19) as well as by a sublimation technique (the result of the present work). On the other hand, slow crystallization from acetonitrile solution results in formation of the new AANP phase (space group $Pca2_1$, $Z=4$) which is very similar to and isostructural with the known COANP structure. So, AANP was found to form at least two non-centrosymmetric polymorphs having different crystal packing arrays. This observation seems to be very important taking into account possible applications of this compound in optical devices. In the present work X-ray diffraction analysis has been performed for both AANP phases obtained by sublimation ($Pna2_1$ phase, diffraction data were collected at room temperature) and by crystallization from the acetonitrile solution (new $Pca2_1$ phase, data were obtained at room temperature and at 163 K to increase accuracy of the diffraction data).

To understand details of the thermal behavior and polymorphism of the compounds studied, we also performed molecular mechanics calculations of the molecular conformations for both compounds. These calculations were done to determine the factors which might be responsible for the glassy state of COANP and possible conformational polymorphism of AANP. Energetic calculations were also performed for the first time to evaluate the crystal morphology of both compounds.

Taking into account that COANP and AANP form different crystal phases on cooling the melts, both linear and quadratic electro-optical (EO) effects for their single crystal films were examined by an ac modulation method using a longitudinal setup. The EO coefficient r_{51} and figures of merit for COANP and AANP were measured and compared.

Calculations and experimental

Molecular mechanics calculations of isolated molecules

The molecular geometry of the COANP and AANP molecules was optimized using standard procedures and parameters

incorporated in the MM3 program package.[27,28] The search for the possible molecular conformations was done with a stochastic search procedure.[29a] This procedure is especially useful when a molecule contains one or more flexible cyclic fragments for which comprehensive conformational analysis (in Hendricson's manner[29b]) is very time consuming. In a stochastic search,[29a] any conformer may be used to initiate the search. The next conformer is generated by a displacement of the atoms in a molecule randomly in a sphere with estimated radii. Then, conformational energy is minimized and the output structure stored. After that, the procedure is repeated using the last structure obtained to generate the next conformer. When difference in the conformational energy is less than 0.053 kcal mol^{-1}, similar conformers (with indication how often this conformer was found) are stored in the same group. The top-list of the calculated energies for COANP and AANP molecules is presented in Table 1. The dependence of the molecular conformational energy on the substituent orientation has also been calculated.

Analysis of crystal morphology

Computational evaluation of the *crystal morphology* has been performed with the NONVPOT program package.[30,31] It is known that crystal shape is determined by the relative rates of deposition of molecules on various faces.[32] For crystals grown at low supersaturating conditions the relative growth rate of a given face is considered to be proportional to the attachment energy defined as the energy per molecule released when a new layer is attached to the surface of the crystal.[33] The atom–atom potential method[34,35] makes possible the calculation of the attachment (or adhesive) energy provided the crystal structure of the compound under investigation is known. As a rule, the most developed crystal faces are coplanar with the molecular layers having the highest intramolecular energy. The approach used for single crystal morphology evaluation is described in detail in refs. 36,37. In our crystal morphology calculations we used the force field developed in ref. 33. Relative crystal face areas for the most developed crystal faces of COANP and two polymorphs of AANP are given in Table 2.

Electro-optical measurements

The AANP and COANP single crystal films were grown by a plate guided (PG) method in a fused quartz cell reported earlier.[26] Indium Tin Oxide (ITO) layers with thickness of *ca.* 240 nm were deposited onto the two inner surfaces of the cell and the lid by (dc) magnetron sputtering of a pressed ITO target in 5 mTorr argon atmosphere. The rf power was 20 W. After deposition, gold wire leads were attached to the terminals of the plates with silver paste.

A cell filled with either AANP or COANP powder was put onto a hot plate, and melted. Precautions were taken to avoid air bubble formation inside the cell. The cell was sealed after the melt cooled. The cell was then put onto a homemade heat exchange chamber on a polarizing microscope in which heated liquid passed through. The melting and recrystallization rates of AANP and COANP varied with the ambient temperature. Only one seed located in the middle of the cell was chosen, and usually several attempts had to be made to get a high-quality single crystal film. The growth rate of the COANP crystal was much slower than that of AANP.

The electro-optic effects were characterized by an ac modulation method similar to that used by Yoshimura.[38] We used longitudinal geometry for evaluation of electrooptical effects, where the applied electric field is parallel to the laser beam. In such geometry, it was possible to evaluate only the r_{51} electrooptical coefficient.[39] The experimental setup for the EO measurements is presented in Fig. 1.

A 632.8 nm He–Ne laser with 2 mW was employed as the light source. Two Glan–Thompson polarizers were used as polarizer and analyzer, and a Fresnel double rhomb (FDR) was used to rotate the plane of polarization. After passing the polarizer and the FDR, the light beam was directed into the cell, then through the analyzer, and was finally detected by a silicon photodetector. The dc beam intensity was monitored by an oscilloscope. A sinusoidal modulated voltage with a frequency of 1 kHz and amplitude up to 9 V was applied to the quartz plates from a function generator. Pockels and Kerr's effects were detected by a lock-in-amplifier and compared with the reference signal at 1 kHz and 2 kHz, respectively. The driving voltage, both dc and ac, was applied to the crystal through the two ITO layers. Maximum efficiency of both effects, linear and quadratic, was observed when the beam was incident into the crystal along the matching condition direction, the same condition as for the second harmonic generation.

X-Ray analysis

The synthesis and purification of COANP and AANP were performed according to ref. 10*a*. Single crystals of COANP and AANP (new $Pca2_1$-phase) suitable for X-ray analysis were obtained by slow crystallization from acetonitrile and had the shape of thin yellow prisms with the approximate dimensions $0.2 \times 0.40 \times 0.40$ mm. The melting point of this phase for AANP was found to be 165 °C. The $Pna2_1$ phase of AANP (thin plates) was obtained by slow sublimation in a sealed tube; these crystals have melting point of 167 °C. Unit cell parameters as well as the melting point of this phase were found to be identical with those for AANP crystal grown by zone melting.[11,19]

Unit cell parameters and intensities of reflections were measured with a 4-circle X-ray diffractometer "Siemens P3/PC" equipped with a low temperature device (for COANP and $Pca2_1$ phase of AANP) and "CAD-4" diffractometer (for $Pna2_1$ phase of AANP) using MoKα radiation and $\theta/2\theta$-scan technique. Experimental details and results of refinements are summarized in Table 3. The quality of the single crystal for the $Pna2_1$ phase of AANP was rather poor; nevertheless the main features of its crystal structure were proven without any doubt. The structures were solved by direct methods and refined by full-matrix least-squares in the anisotropic approximation for the non-hydrogen atoms. All hydrogen atoms were located from the difference Fourier-synthesis and included in the final

Table 1 Top-list energies (U_{conf}/kcal mol^{-1}) for molecular conformations of COANP and AANP found by stochastic search, and torsion angles (ρ_1 and ρ_2/deg) characterizing corresponding conformations

COANP				AANP			
Conformation	ρ_1/deg	ρ_2/deg	U_{conf}/kcal mol^{-1}		ρ_1/deg	ρ_2/deg	U_{conf}/kcal mol^{-1}
1	−0.5	145.9	25.15	1	0.0	180.0	24.18
2	−0.8	153.7	25.22	2	0.4	−141.4	25.96
3	−0.3	126.6	25.29	3	0.0	−136.0	26.03
4	0.2	115.3	25.47				
5	0.3	71.2	26.02				
6	0.2	62.7	26.25				

Table 2 Relative surface areas for the most developed faces of COANP and AANP

COANP		AANP, $Pca2_1$		AANP, $Pna2_1$	
Face index	Relative area	Face index	Relative area	Face index	Relative area
(100)	2.50	(100)	3.52	(010)	2.61
(011)	1.69	(110)	1.63	(001)	2.91
(110)	1.78	(101)	1.00	(00 −1)	4.20
(10 −1)	2.01	(10 −1)	1.77	(110)	2.05
Crystal surface area	23.17		23.57		23.52

refinements using the "riding" model (room temperature data) or in the isotropic approximation (low temperature data). All calculations were performed with a PC computer using the SHELXTL PLUS program package.[40] A general view of the COANP and AANP molecules with the atoms shown as 50% probability thermal ellipsoids and atomic numbering schemes are given in Figs. 2 and 3. Full crystallographic details have been deposited at the Cambridge Crystallographic Data centre (CCDC). Important bond lengths and bond angles (for the low temperature data only) are presented in Tables 3–5.

Results and discussion

Molecular geometry and crystal packing†

Bond lengths and bond angles in the COANP and AANP molecules for the more accurate low temperature data are presented in Tables 4 and 5. Molecular geometry parameters are not unexceptional; nevertheless several interesting features should be noted. In particular, a remarkable quinoid character in the pyridine ring bond length distribution was found in both structures with partial double bond character for N(1)–C(5), C(2)–C(3) and C(1)–N(2) bonds. This may indicate that the charge transfer direction for these molecules mostly takes place along the N(2)···N(3) vectors. Our quantum chemical AM1 calculations (MOPAC[42]) have demonstrated that the dipole moment directions for the molecules studied are very close to these vectors (the difference does not exceed 5–7°). Calculated values for the dipole moments were found to be 8.27 D for COANP and 7.45 D for AANP, respectively.

The nitro groups in both structures are almost in the ring planes (interplanar angles are equal to 7.4° for COANP and 4.2° for AANP), and the N(2)-amino nitrogens have almost planar bond configuration (the sum of the bond angles are 360.0 and 358.8°, respectively). The planes of the amino groups are not exactly in the ring planes and corresponding torsion angles N(1)–C(1)–N(2)–C(6) in the COANP and AANP molecules are equal to −6.5 and −10.0°. The larger value of this angle for AANP is probably related to the larger volume of the bulky adamantyl substituent. This is evidenced as well in the larger C(1)–N(2)–C(6) bond angle for AANP (128.7 and 125.4°, respectively).

Crystal packing diagrams for COANP and AANP (for each of the crystal phases) are presented in Fig. 4 in the projections which most easily enable comparison. It is seen that for the COANP and AANP ($Pca2_1$) phases these diagrams are very similar. Taking into account very close unit cell parameters for both compounds (Table 3) we may conclude that they are "isostructural". In these two crystals, molecules form endless "double" layers perpendicular to the longest crystal *a*-axes and separated by the hydrophobic cyclooctyl and adamantyl substituents. So, the cleavage plane for these crystals most probably will be (100), *i.e.* the *bc*-plane that was proven for COANP experimentally.[10b] Along the polar *c*-axes, the COANP and AANP molecules form infinite chains. These are formed by the hydrogen bonds N(2)–H···O(1′) between the amino nitrogen N(2) and the oxygen O(1′) atom of the nitro group [atom O(1′) is related to the basis O(1) one by the symmetrical transformation $1/2-x$, $1+y$, $1/2+z$]. Geometric parameters of these H-bonds are: H···O 2.15 and 1.89 Å, N–H–O angles 169 and 171°, N···O 2.995(6) and 2.964(2) Å for COANP and AANP (for the low-temperature $Pca2_1$ phases), respectively. So, taking into account the N···O distances, the hydrogen bond in AANP seems to be a little stronger than in COANP. It is interesting to note that for both structures there is a small but significant non-equivalence between the N–O bond lengths for the nitro groups: the O(1)–N(3) bonds are consistently longer than the O(2)–N(3) bonds (see Tables 4 and 5) because of participation of the O(1) atoms in hydrogen bonds.

The orientation of the molecular dipoles in the $Pca2_1$ phase for both COANP and AANP with respect to polar axes was found to be very close to the "optimal" value of 54.74° for efficient phase matching SHG for crystals with the *mm*2 symmetry.[6] In particular, the angles between the polar crystal *c*-axes and the molecular dipole moments are equal to 60.1° for COANP and 58.3° for AANP, respectively. The mutual orientation of the molecular dipoles is of a herring-bone type with a relative shift of neighboring layers, so it may be defined more correctly as a "parquet-like" packing (Fig. 5). This kind of molecular dipole arrangement is quite usual for organic NLO materials. Taking into account that both compounds have relatively high molecular second-order hyperpolarizabilities (calculated β values are equal to 33.9 and 34.3×10^{-51} $Cm^3\,V^{-2}$, respectively for COANP and AANP; calculations were based on the X-ray geometry using the MOPAC and HYPER programs[42]), we may expect that the new $Pca2_1$-phase of AANP must possess quite large NLO responses in the solid state. However, optical studies of this phase have not been reported.

Another type of crystal packing was found in the $Pna2_1$ phase of AANP (Fig. 4). In this crystal, molecules also form layers along the polar *c*-axis formed by the same type of N–H···O hydrogen bonds (N···O 3.063 Å, symmetry transformation $-1/2+x$, $1/2-y$, $-1+z$), but these H-bonds are a little longer than in both $Pca2_1$-phases of the COANP and AANP (2.995 and 2.964 Å, respectively). The layers are separated by the adamantyl substituents and are perpendicular to the longest crystal *b*-axis. The most important difference between the phases studied is the mutual orientation of the molecular dipoles along the polar crystal axes. In the $Pna2_1$ phase of AANP the dipoles form an "ideal" herring-bone array without a relative shift of neighboring layers as was found in the $Pca2_1$

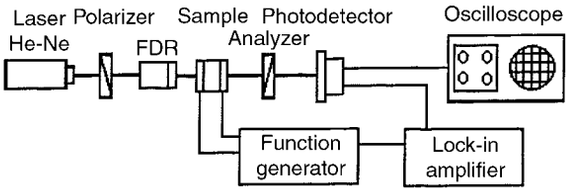

Fig. 1 Schematic diagram of the EO measurements system.

†CCDC reference number 1145/263. See http://www.rsc.org/suppdata/jm/b0/b005822j/ for crystallographic files in .cif format.

Table 3 Structure determination summary for COANP and AANP

	COANP (298 K)	COANP (167 K)	AANP (163 K, $Pca2_1$)	AANP (298 K, $Pca2_1$)	AANP (298 K, $Pna2_1$)
Empirical formula	$C_{13}H_{19}N_3O_2$	$C_{13}H_{19}N_3O_2$	$C_{15}H_{19}N_3O_2$	$C_{15}H_{19}N_3O_2$	$C_{15}H_{19}N_3O_2$
Formula weight	249.31	249.31	273.33	273.33	273.33
Crystal system	Orthorhrombic	Orthorhombic	Orthorhrombic	Orthorhombic	Orthorhombic
Space group, Z	$Pca2_1$, 4	$Pca2_1$, 4	$Pca2_1$, 4	$Pca2_1$, 4	$Pca2_1$, 4
Unit cell dimensions					
a/Å	26.285(5)	26.099(5)	28.158(6)	28.310(10)	7.991(2)
b/Å	6.647(1)	6.637(2)	6.584(2)	6.612(2)	26.326(6)
c/Å	7.631(2)	7.555(2)	7.395(1)	7.474(2)	6.588(1)
Volume/Å^3	1333.3(5)	1308.7(6)	1371.0(5)	1398.9(7)	1385.9(5)
Density (calc/g cm^{-3})	1.242	1.265	1.324	1.298	1.310
Abs. coeff./cm^{-1}	0.86	0.87	0.90	0.88	0.89
F(000)	536	536	584	584	584
θ range/deg	3.06–27.57	1.56–27.55	1.45–40.09	1.44–27.05	2.66–24.96
Scan range (ω/deg)	1.90	1.90	1.80	1.90	1.90
Independent refls.	1657	1622	4242	1645	1322
Obs. refls. ($I>2\sigma(I)$)	847	915	2919	565	329
No. of param. refined	163	163	257	185	181
Final R_1 (obs. data)[a]	0.0736	0.0592	0.0513	0.0719	0.0659
Final wR_2 (all data)[b]	0.2592	0.1637	0.1535	0.4079	0.2310
Goodness of fit	1.068	1.021	1.022	1.008	0.863
Absolute structure param.[c]	−1(5)	1(3)	0.9(13)	1(6)	5(5)

[a] $R_1=\sum||F_o|-|F_c||/\sum(F_o)$. [b] $wR_2=\{\sum[w(F_o^2-F_c^2)^2]/\sum w(F_o^2)^2\}1/2$. [c] Flack absolute structure parameter x.[41]

phases. Moreover, the angle between the AANP molecular dipole and the polar crystal axis in the $Pna2_1$ phase is equal to only 39.1°. Nonlinear optical (SHG) properties of this phase (large single crystals were grown by a zone-melting technique) were first studied in ref. 11 and it was established by the SHG measurements at 1064 nm that the d_{31} and d_{33} coefficients are rather large and equal to 80 and 60 pm V^{-1}, respectively, and therefore AANP was considered to be a very promising material for Type II angle-tuned phase-matched wavelength conversion with high efficiency in the optical communications wavelength region. We must note, however, that the authors[11] (see also refs. 19,20) were not aware that they were working with the "non-optimal" $Pna2_1$ phase of AANP, where the angle between the polar axis and charge transfer (molecular dipole moment) direction is equal to 39.1° only. The partial crystal packing diagram for the AANP structure along the c-axis given in ref. 11 corresponds to the $Pna2_1$ space group; however during interpretation of the large NLO responses of this phase the authors used the wrong molecular orientation angle (58° instead of the experimental value 39.1°).

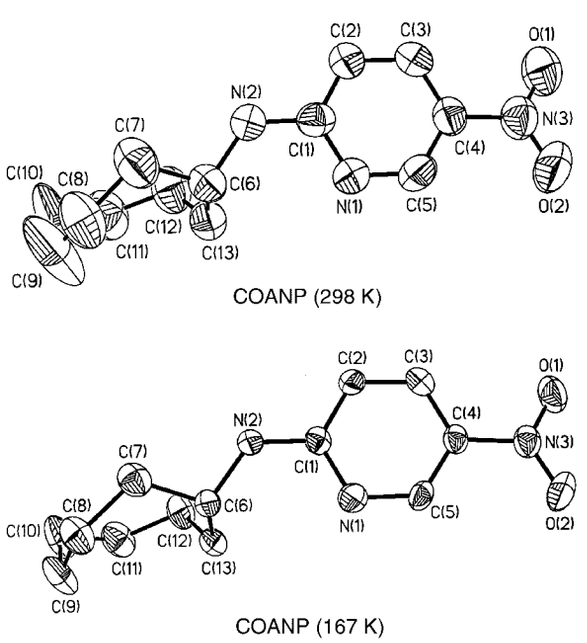

Fig. 2 General view of the COANP molecule with the atoms shown as thermal ellipsoids at 298 K and 167 K.

Molecular conformation calculations

Detailed calculations of the molecular conformations of COANP and AANP have been performed to reveal the conformational features of these two molecules. As expected, the conformational behavior of COANP and AANP is different. In particular, for COANP the calculation of the conformation energy dependence on the torsion angle N(1)–C(1)–N(2)–C(6) (ρ_1) shows two low energy areas, and only restricted rotation around the C(1)–N(2) bond due to the bulky cyclooctyl substituent is permitted for this molecule. A stochastic conformational search in the vicinity of the region with $\rho_1=0°$ gives several possible positions of the cyclooctyl ring (torsion angle ρ_2 = C(1)–N(2)–C(6)–C(7)). Conformations corresponding to the first two local minima in this calculation ($\rho_2=145.9$ and 153.7°, see Table 1) are close to those found in the crystal ($\rho_2=159.1°$). Analysis of the cyclooctyl ring conformations obtained by the stochastic search procedure shows that in all cases the ring conformation is the boat–chair (BC), which corresponds to that found in the crystal at both temperatures (Fig. 6). The same conformation was indicated by several authors as corresponding to the lowest energy for the cyclooctane ring.[43] In the gas phase (according to the electron diffraction data for cyclooctane) coexistence of the two twist–

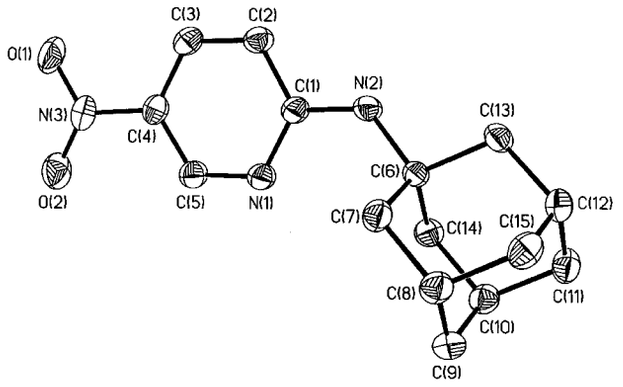

Fig. 3 General view of the AANP molecule with the atoms shown as thermal ellipsoids (data at 163 K).

Table 4 Bond lengths (Å) and angles (deg.) for COANP at 167 K

O(1)–N(3)	1.242(4)	C(5)–N(1)–C(1)	117.2(3)
O(2)–N(3)	1.222(4)	C(1)–N(2)–C(6)	125.3(3)
N(1)–C(5)	1.322(4)	O(2)–N(3)–O(1)	121.9(3)
N(1)–C(1)	1.356(4)	O(2)–N(3)–C(4)	120.1(3)
N(2)–C(1)	1.336(4)	O(1)–N(3)–C(4)	118.0(3)
N(2)–C(6)	1.471(4)	N(2)–C(1)–N(1)	118.3(3)
N(3)–C(4)	1.427(5)	N(2)–C(1)–C(2)	119.7(3)
C(1)–C(2)	1.421(5)	N(1)–C(1)–C(2)	121.9(3)
C(2)–C(3)	1.351(5)	C(3)–C(2)–C(1)	119.7(3)
C(3)–C(4)	1.396(5)	C(2)–C(3)–C(4)	117.8(4)
C(4)–C(5)	1.381(5)	C(5)–C(4)–C(3)	119.7(3)
C(6)–C(7)	1.523(5)	C(5)–C(4)–N(3)	120.1(3)
C(6)–C(13)	1.524(5)	C(3)–C(4)–N(3)	120.2(3)
C(7)–C(8)	1.520(5)	N(1)–C(5)–C(4)	123.6(3)
C(8)–C(9)	1.525(6)	N(2)–C(6)–C(7)	106.5(3)
C(9)–C(10)	1.510(6)	N(2)–C(6)–C(13)	109.7(3)
C(10)–C(11)	1.503(6)	C(7)–C(6)–C(13)	115.9(3)
C(11)–C(12)	1.535(6)	C(8)–C(7)–C(6)	117.5(3)
C(12)–C(13)	1.540(6)	C(7)–C(8)–C(9)	118.2(4)
		C(10)–C(9)–C(8)	116.4(4)
		C(11)–C(10)–C(9)	117.0(4)
		C(10)–C(11)–C(12)	118.9(4)
		C(11)–C(12)–C(13)	116.2(3)
		C(6)–C(13)–C(12)	114.7(3)

chair–boat (TCB) and twist–boat–chair (TBC) conformations has been found for this flexible ring.[44]

The distinction between the calculated low energy conformations of COANP may be described as follows. In the calculated conformations 1–4 (Table 1) the N(2)–C(6) bond is attached to the C(6) atom of the ring that corresponds to the ideal position 2 in the BC-conformation,[43] and therefore this conformation corresponds to that found in the crystal. So, all conformations 1–4 may be considered as belonging to a one broad energetic minimum. On the contrary, conformations 5 and 6 belong to the other different minima inspite of the similarityof the torsion angles ρ_1 and ρ_2.

In conformation 5 the same bond is attached to atoms analogous to the C(9) or C(13) (position 3 in the BC), and in the conformation 6 it is attached to the atom analogous to the C(7) (position 1 in the BC). Thus, our calculations show that the orientational flexibility (rotation around the C(1)–N(2) bond) of the COANP molecule coexists with the ring flexibility. Both of these circumstances might be the reason for the formation of a glassy state of COANP on cooling the melt because of the co-existence of many molecular conformations in the melt having nearly the same energy, and the crystal structure disorder at room temperature. Nevertheless, no new crystal phases (polymorphism) were detected for COANP. It may be seen from Fig. 2 that at room temperature atomic thermal ellipsoids in COANP are very large indicating some kind of nonresolved crystal disorder. This disorder results only in the effective shortening of the single C–C bond lengths in the ring (for instance, single C(10)–C(11) and C(12)–C(13) bonds are as short as 1.42 Å), and strong molecular non-rigidity (rigid-body test resulted in the very large R_u value of 0.29). We could not, however, split atomic positions of the disordered atoms. On the other hand, on cooling the crystal, the ellipsoid size decreases almost linearly with temperature, which might be an indication of the dynamic nature of the disorder related to the large flexibility of the cyclooctane ring. The rigid-body test for the whole molecule at 163 K was found to be much more satisfactory ($R_u = 0.16$).

In the case of AANP it is quite possible that this molecule is significantly less flexible than COANP because of the rigidity of the adamantyl substituent. Our calculations show that reorientation of this substituent is possible around the C(1)–N(2) bond (torsion ρ_1 angle N(1)–C(1)–C(2)–C(6) is in the range -60 to $+60°$), and substituent rotation is possible around the N(2)–C(6) bond (torsion angle ρ_2 = C(1)–N(2)–C(6)–C(7)) with a barrier of about 2 kcal mol^{-1}. These observations make possible conformational polymorphism for AANP as well. We found experimentally that in the two AANP polymorphs the molecules have the same but slightly differing conformations: torsion ρ_1 angles in the $Pca2_1$ and $Pna2_1$ phases are equal to 10.2 and 3.0°, respectively. However, this difference seems to be too small to explain the polymorphism of AANP.

Table 5 Bond lengths (Å) and angles (deg.) for AANP ($Pca2_1$ phase at 163 K)

O(1)–N(3)	1.244(2)	C(5)–N(1)–C(1)	117.54(13)
O(2)–N(3)	1.223(2)	C(1)–N(2)–C(6)	128.68(12)
N(1)–C(5)	1.328(2)	O(2)–N(3)–O(1)	122.5(2)
N(1)–C(1)	1.354(2)	O(2)–N(3)–C(4)	120.07(14)
N(2)–C(1)	1.346(2)	O(1)–N(3)–C(4)	117.4(2)
N(2)–C(6)	1.472(2)	N(2)–C(1)–N(1)	119.35(13)
N(3)–C(4)	1.433(2)	N(2)–C(1)–C(2)	118.20(13)
C(1)–C(2)	1.426(2)	N(1)–C(1)–C(2)	122.43(14)
C(2)–C(3)	1.362(2)	C(3)–C(2)–C(1)	119.04(14)
C(3)–C(4)	1.399(2)	C(2)–C(3)–C(4)	117.88(13)
C(4)–C(5)	1.387(2)	C(5)–C(4)–C(3)	120.19(14)
C(6)–C(14)	1.536(2)	C(5)–C(4)–N(3)	119.57(14)
C(6)–C(13)	1.538(2)	C(3)–C(4)–N(3)	120.15(13)
C(6)–C(7)	1.539(2)	N(1)–C(5)–C(4)	122.9(2)
C(7)–C(8)	1.534(2)	N(2)–C(6)–C(14)	112.29(12)
C(8)–C(9)	1.532(3)	N(2)–C(6)–C(13)	105.81(10)
C(8)–C(15)	1.535(2)	C(14)–C(6)–C(13)	108.70(12)
C(9)–C(10)	1.527(3)	N(2)–C(6)–C(7)	110.91(12)
C(10)–C(11)	1.535(2)	C(14)–C(6)–C(7)	110.06(12)
C(10)–C(14)	1.537(2)	C(13)–C(6)–C(7)	108.92(13)
C(11)–C(12)	1.532(2)	C(8)–C(7)–C(6)	109.67(12)
C(12)–C(13)	1.535(2)	C(9)–C(8)–C(7)	109.4(2)
C(12)–C(15)	1.535(2)	C(9)–C(8)–C(15)	109.63(14)
		C(7)–C(8)–C(15)	109.34(13)
		C(10)–C(9)–C(8)	109.78(13)
		C(9)–C(10)–C(11)	109.4(2)
		C(9)–C(10)–C(14)	109.90(13)
		C(11)–C(10)–C(14)	109.55(13)
		C(12)–C(11)–C(10)	109.22(12)
		C(11)–C(12)–C(13)	109.26(14)
		C(11)–C(12)–C(15)	109.81(14)
		C(13)–C(12)–C(15)	109.69(13)
		C(12)–C(13)–C(6)	109.83(11)
		C(6)–C(14)–C(10)	109.24(12)
		C(12)–C(15)–C(8)	109.04(13)

Evaluation of the crystal morphology

Relative surface areas of the most important calculated crystal faces are summarized in Table 2. In the crystals of COANP and AANP ($Pca2_1$ phases) the most developed faces are (100) and (−100) which are parallel to the molecular layers and perpendicular to the longest unit cell parameters. All other faces are less developed, especially for the AANP crystal. As we noted before, this phase of AANP might possess rather large NLO responses because of optimal molecular orientation with respect to the more developed crystal face. The situation somewhat differs from that for the AANP $Pna2_1$ phase where molecular layers are perpendicular to the crystal *b*-axis. According to our calculations, the more developed faces in this phase are perpendicular to the *b*-axis and perpendicular to the *c*-axis, as well as in the diagonal (110) direction. This result may indicate that a variation of the crystal growth conditions will allow one to obtain bulk crystals or thin films with different molecular orientations for desirable NLO applications. In particular, our experimental EO measurements for COANP and AANP thin films (see below) are in a good agreement with these expectations.

Electro-optical effects

The measured phase shifting $\Delta\delta$, figures of merit *F*, and electro-optical coefficient r_{51} are given in Table 6.

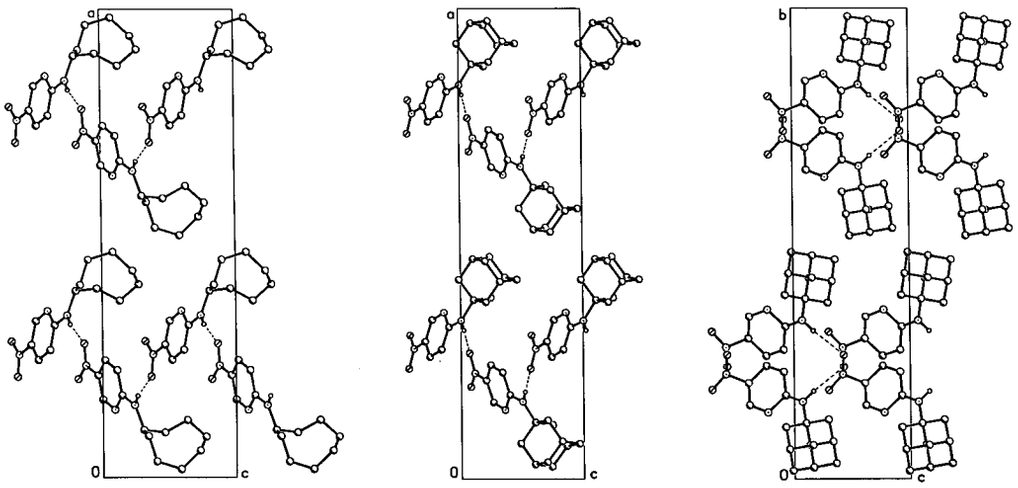

Fig. 4 Crystal packing diagrams for the $Pca2_1$ phases of COANP and AANP, and $Pna2_1$ phase of AANP. Projections are given in the planes containing the polar *c*-axes.

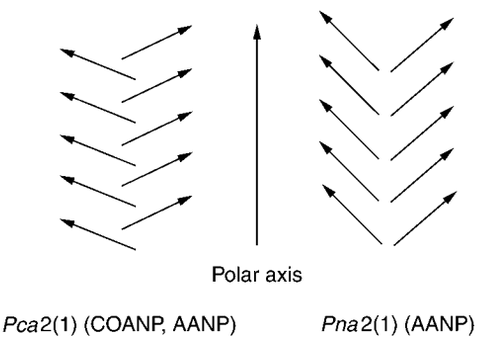

Fig. 5 Scheme of the molecular dipole orientation with respect to the polar crystal axes for the $Pca2_1$ (COANP, AANP) and $Pna2_1$-phases (AANP).

Both crystal films exhibited the Pockels effect, but the AANP did not reveal any quadratic response. Our data also showed that the measured electro-optical r_{51} coefficients for both crystals are lower than the r_{i3} ones ($i=1$–3) obtained from the transverse measurements[14] for COANP. The EO measurements for AANP are lacking in the literature. The most interesting is the large difference (2.48 and 0.63 pV m^{-1}, the ratio 3.94) between the r_{51} coefficients for AANP and COANP, respectively. We assume that this difference may be attributed to the different crystal structure of the films used for EO measurements. In particular, on cooling the melts, COANP forms the $Pca2_1$ phase, while AANP forms the $Pna2_1$ phase which differs from the first one by the orientation angle θ_p between the molecular charge transfer direction and the polar crystal axes ($\theta_p=39.1$ and 58.3° for AANP and COANP, respectively obtained from melts). It is known[2] that in the "optimal" crystal for the EO-effect, the value of θ_p must be equal to zero, and therefore the $\cos^3\theta_p$ value indicates the decrease in the electro-optical coefficient compared to an ideal arrangement of the molecules in the crystal lattice (neglecting possible local field effects). In our case, the ratio $\cos^3\theta_p$(AANP)/$\cos^3\theta_p$(COANP) was found to be 3.77 which is very close to the ratio of corresponding r_{51} coefficients (3.94).

Table 6 Measured optical characteristics for COANP and AANP crystals

	Phase shifting ($\Delta\delta$)	Figure of merit, F/pm V^{-1}	r_{51}/pm V^{-1}
COANP	2.5×10^{-4}	4.2	0.63
AANP	5.8×10^{-4}	10.7	2.48

Concluding remarks

In the present paper we have demonstrated that the crystals of AANP form two polymorphic modifications obtained by crystallization from solution ($Pca2_1$ phase) and from the melt or the gas phase ($Pna2_1$ phase). The $Pca2_1$ phase of AANP has not been reported before, and it was found that it is isostructural with the known COANP structure. In accord with molecular crystal packing analysis for both phases of AANP, the $Pca2_1$ phase may be an even more active SHG material compared to the $Pna2_1$ phase studied earlier. Molecular mechanics conformational, as well as crystal morphology calculations have been performed for both compounds, and were found to be in good agreement with the experimental data. Electro-optical effects for the single crystal films for both compounds were examined, and the difference between the measured r_{51} coefficients was explained by the different molecular orientation in both crystals. Our new structural data about two different polymorphic phases of the compounds studied allowed one also to give an explanation for significantly different values of the measured d_{31} and d_{33} coefficients for AANP (80 and 60 pm V^{-1}) and COANP (15 and 10 pm V^{-1}, respectively[2]) despite their very similar

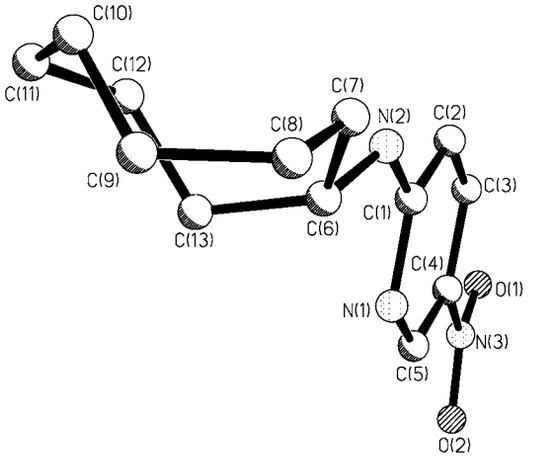

Fig. 6 General view of the COANP molecule in the crystal demonstrating the conformation of the cyclooctyl ring.

molecular hyperpolarizabilities (see above) which is related most probably to the different molecular orientation in these phases.

Our results on polymorphism of AANP demonstrate also that searching for new polymorphs among potential NLO materials might be an easy and feasible way to discover them. Most probably, there exist many more still undetected and new crystal phases among the organic chromophoric compounds studied, especially those possessing some conformational flexibility. In particular, as many as six solvent-free polymorphs, which differ in the mode of packing and in molecular conformation, were found recently for 5-methyl-2-[(2-nitrophenyl)amino]thiophene-3-carbonitrile.[45] This very new and interesting example (according to the Cambridge Structural Database, so many different crystal modifications for a single compound have not previously been reported in the literature) may demonstrate once again that the "…number of (crystal) forms for a given compound is proportional to the time and energy spent in research on that compound".[46]

Acknowledgements

This work was supported by AFOSR Grant (F49620-97-1-0256) and in part by NASA Grant (NAG5-6532).

References

1 S. P. Karna and A. T. Yeates, 'Nonlinear Optical Materials, Theory and Modeling', *ACS Symp. Ser. 628*, Washington, DC, 1996.
2 H. S. Nalwa and S. Miyata, *Nonlinear Optics of Organic Molecules and Polymers*, CRC Press, Boca Raton, New York, London, Tokyo, 1997.
3 M. G. Kuzyk and C. W. Dirk, *Characterization Techniques and Tabulations for Organic Nonlinear Optical Materials*, Marcel Dekker, Inc., New York, Basel, Hong Kong, 1998.
4 G. R. Desiraju, *Acc. Chem. Res.*, 1996, **29**, 441.
5 G. R. Desiraju, *Angew. Chem., Int. Ed. Engl.*, 1995, **34**, 2311.
6 J. Zyss, I. Ledoux and J.-F. Nicoud, *Molecular Nonlinear Optics*, Academic Press Inc. Harcourt Brace and Company, San Diego, London, 1994, pp. 129–200.
7 M. C. Etter and G. M. Frankenbach, *Chem. Mater.*, 1989, **1**, 10.
8 S. J. Geib, S. C. Hirst, C. Vicent and A. D. Hamilton, *J. Chem. Soc., Chem. Commun.*, 1991, 1283.
9 R. W. Munn and M. Hurst, *Chem. Phys.*, 1990, **147**, 35.
10 (*a*) P. Günter, Ch. Bosshard, K. Sutter and H. Arend, *Appl. Phys. Lett.*, 1987, **50**(9), 486; (*b*) Ch. Bosshard, K. Sutter, P. Günter and G. Chapuls, *J. Opt. Soc. Am. B.*, 1989, **6**(4), 721.
11 S. Tomary, S. Matsumoto, T. Kirihara, H. Suzuki, N. Ooba and T. Kaino, *Appl. Phys. Lett.*, 1991, **58**(23), 2583.
12 J.-F. Nicoud, 'Nonlinear Optical Properties of Organic Materials', *Proc. SPIE—Int. Soc. Opt. Eng.*, 1988, **971**, 68.
13 Y. Le Fur, M. Bagieu-Beucher, R. Masse, J.-F. Nicoud and J.-P. Levy, *Chem. Mater.*, 1996, **8**, 68.
14 Ch. Bosshard, K. Sutter, R. Schlesser and P. Günter, in 'Nonlinear Optical Properties of Organic Materials', *Proc. SPIE—Int. Soc. Opt. Eng.*, 1992, **1775**, pp. 271–282.
15 J. Pecaut, J. P. Levy and R. Masse, *J. Mater. Chem.*, 1993, **3**(10), 999.
16 M. Eich, H. Looser, D. Y. Yoon, R. Twieg, G. Bjorklund and J. C. Baumert, *J. Opt. Soc. Am. B*, 1989, **6**(8), 1590.
17 K. Sutter and P. Gunter, *J. Opt. Soc. Am. B*, 1990, **7**(12), 2274.
18 G. Lahanar, I. Zupancic, R. Blinc, A. Zidansek, R. Kind and M. Z. Ehrensperger, *Z. Phys. B*, 1994, **B95**, 243.
19 A. Yokoo, S. Tomaru, I. Yokohama, H. Itoh and T. Kaino, *J. Cryst. Growth*, 1995, **156**, 279.
20 A. Yokoo, I. Yokohama, H. Takara and T. Kaino, *Proc. SPIE—Int. Soc. Opt. Eng.*, 1997, **3147**, 20.
21 C. B. Aakeroÿ, A. M. Beatty, M. Nieuwenhuyzen and M. Zou, *J. Mater. Chem.*, 1998, **8**(6), 1385.
22 C. Serbutoeviez, J.-F. Nicoud, J. Fischer, I. Ledoux and I. Zyss, *Chem. Mater.*, 1994, **6**(8), 1358.
23 H. Kagawa, M. Sagawa, T. Hamada, A. Kakuta, M. Kaji, H. Nakayama and K. Ishii, *Chem. Mater.*, 1996, **8**, 2622.
24 F. Pan, C. Bossard, M. S. Wong, C. Serbutoviez, K. Schenk, V. Gramlich and P. Günter, *Chem. Mater.*, 1997, **9**, 1328.
25 (*a*) C. B. Aakeroÿ, M. Nieuwenhuyzen and S. L. Price, *J. Am. Chem. Soc.*, 1998, **120**, 8986; (*b*) J. Bernstein, R. J. Davey and J.-O. Henck, *Angew. Chem., Int. Ed.*, 1999, **38**, 3440.
26 A. Leyderman, M. Espinosa, T. Timofeeva, R. Clark, D. Frazier and B. Penn, *Proc. SPIE—Int. Soc. Opt. Eng.*, 1996, **2809**, 144.
27 N. L. Allinger and J.-H. Lii, *J. Am. Chem. Soc.*, 1989, **111**, 8551.
28 J.-H. Lii and N. L. Allinger, *J. Am. Chem. Soc.*, 1989, **111**, 8566.
29 (*a*) M. Saunders, *J. Am. Chem. Soc.*, 1987, **109**, 3150; (*b*) J. B. Hendricson, *J. Am. Chem. Soc.*, 1973, **86**, 4854.
30 V. I. Shil'nikov, *Kristallografia.*, 1994, **39**, 647.
31 T. V. Timofeeva, V. I. Shil'nikov and R. D. Clark, *Proc. SPIE—Int. Soc. Opt. Eng.*, 1997, **3123**, 159.
32 P. Hartman and P. Bonnema, *J. Cryst. Growth*, 1980, **49**, 157.
33 A. Gavezzotti and G. Filippini, *J. Phys. Chem.*, 1994, **98**, 4831.
34 A. I. Kitaigorodsky, *Molecular Crystals and Molecules*, Academic Press, New York, 1973.
35 A. J. Pertsin and A. I. Kitaigorodsky, *Atom–Atom potential Method. Application to Organic Molecular Solids*, Springer Verlag, Berlin, Heidelberg, New York, 1987.
36 Z. Berkovitch-Yellin, *J. Am. Chem. Soc.*, 1985, **107**, 8239.
37 G. Clydesdale, K. J. Roberts and R. Docherty, *J. Cryst. Growth*, 1996, **166**, 78.
38 T. Yoshimura, *J. Appl. Phys.*, 1987, **62**(5), 2028.
39 A. Leyderman and Y. Cui, *Opt. Lett.*, 1988, **23**(12), 909.
40 G. M. Sheldrick, SHELXTL/PC, Version 5.02, 1994, Siemens Analytical X-Ray Instruments Inc., Karlsruhe, Germany,
41 H. D. Flack, *Acta Crystallogr., Sect. A*, 1983, **39**, 876.
42 B. H. Cardelino, C. E. Moore and R. E. Stuckel, *J. Phys. Chem.*, 1991, **95**, 8645.
43 U. Burkert and N. L. Allinger, *Molecular Mechanics*, ACS Monogr. 177, ACS, Washington, DC, 1982.
44 O. V. Dorofeeva, V. S. Mastryukov, N. L. Allinger and A. Almenningen, *J. Phys. Chem.*, 1990, **94**, 8044.
45 Y. Lian, G. A. Stephenson, C. A. Mitchell, C. A. Bunnell, S. V. Snorek, J. J. Bowyer, T. B. Borchhardt, J. C. Stowell and S. R. Byrn, *J. Am. Chem. Soc.*, 2000, **122**, 585.
46 W. C. McCrone, *Physics and Chemistry of the Organic Solid State*, Interscience, New York, 1963, vol. 1, p. 725.